J Neurooncol (2017) 135:119–127
DOI 10.1007/s11060-017-2556-z

CLINICAL STUDY

# Temporal evolution of perfusion parameters in brain metastases treated with stereotactic radiosurgery: comparison of intravoxel incoherent motion and dynamic contrast enhanced MRI

**Anish Kapadia[1] · Hatef Mehrabian[2] · John Conklin[1] · Sean P. Symons[1] · Pejman J. Maralani[1] · Greg J. Stanisz[2] · Arjun Sahgal[3] · Hany Soliman[3] · Chinthaka C. Heyn[1,2]**

Received: 3 December 2016 / Accepted: 27 June 2017 / Published online: 1 July 2017


**Abstract** Intravoxel incoherent motion (IVIM) is a magnetic resonance imaging (MRI) technique that is seeing increasing use in neuro-oncology and offers an alternative to contrast-enhanced perfusion techniques for evaluation of tumor blood volume after stereotactic radiosurgery (SRS). To date, IVIM has not been validated against contrast enhanced techniques for brain metastases after SRS. In the present study, we measure blood volume for 20 brain metastases (15 patients) at baseline, 1 week and 1 month after SRS using IVIM and dynamic contrast enhanced (DCE)-MRI. Correlation between blood volume measurements made with IVIM and DCE-MRI show poor correlation at baseline, 1 week, and 1 month post SRS ($r=0.33$, 0.14 and 0.30 respectively). At 1 week after treatment, no significant change in tumor blood volume was found using IVIM or DCE-MRI ($p=0.81$ and 0.41 respectively). At 1 month, DCE-MRI showed a significant decrease in blood volume ($p=0.0002$). IVIM, on the other hand, demonstrated the opposite effect and showed a significant increase in blood volume at 1 month ($p=0.03$). The results of this study indicate that blood volume measured with IVIM and DCE-MRI are not equivalent. While this may relate to differences in the type of perfusion information each technique is providing, it could also reflect a limitation of tumor blood volume measurements made with IVIM after SRS. IVIM measurements of tumor blood volume in the month after SRS should therefore be interpreted with caution.

**Keywords** Stereotactic radiosurgery · Brain metastases · Perfusion magnetic resonance imaging · Dynamic contrast enhanced · Intravoxel incoherent motion · Diffusion weighted magnetic resonance imaging

## Introduction

Stereotactic radiosurgery (SRS) has become standard of practice for treating oligometastatic disease to the brain because of a lower risk of neurocognitive decline and better quality of life indicators as compared to whole brain radiation therapy alone or in combination with SRS [1]. The radiobiology of single fraction high dose radiation and how this ultimately leads to tumor cell death is an evolving area of study and much of what is known about this has come from studies of xenograft models [2, 3]. While conventional fractionated radiation therapy (1.5–2 Gy/fraction) results in an initial increase in tumor perfusion early in the course of treatment with return to or reduction below pre-treatment levels later in treatment [4, 5], SRS results in a profound reduction in tumor blood flow resulting from endothelial injury which occurs in the hours to days after therapy [2, 3] and is hypothesized to play a critical role in the biological response of metastases to SRS [6, 7]. To date, the majority of human studies that have evaluated changes to tumor perfusion after SRS have done so at time points several weeks to months after treatment [8–10] and there is a paucity of data examining early changes in the first month after SRS.

Contrast enhanced techniques such as dynamic susceptibility contrast (DSC) and dynamic contrast enhanced

✉ Chinthaka C. Heyn
chris.heyn@mail.utoronto.ca

[1] Department of Medical Imaging, Sunnybrook Health Sciences Centre and University of Toronto, 2075 Bayview Ave., Toronto, ON M4N 3M5, Canada

[2] Physical Sciences, Sunnybrook Research Institute, Toronto, ON, Canada

[3] Department of Radiation Oncology, Sunnybrook Odette Cancer Center, University of Toronto, Toronto, ON, Canada

(DCE)-MRI are commonly used clinically to evaluate tumor perfusion. DCE-MRI can provide measurements of important tumor perfusion parameters including plasma volume fraction ($v_p$), volume transfer constant ($K^{trans}$) and extravascular extracellular space volume fraction ($v_e$) which relate to blood volume, vascular permeability and tumor extracellular space respectively. In addition to contrast enhanced perfusion techniques, there is growing interest in perfusion methodologies for evaluating tumors which do not require administration of intravenous contrast [9, 11]. This interest has arisen mainly because of safety concerns regarding administration of gadolinium contrast, particularly in oncology patients that require repeat contrast enhanced studies [12]. Intravoxel incoherent motion (IVIM) is an example of a non-contrast perfusion methodology which utilizes differences in diffusion signal between intravascular and extravascular water to calculate blood volume [13, 14]. This technique has recently garnered increasing attention for measuring blood perfusion in CNS diseases including brain tumors [15–18] and has shown promise in detecting very early changes in tumor perfusion in extracranial malignancies treated with therapies targeting tumor blood flow [19].

Given the favorable safety profile of the IVIM methodology, which allows multiple measurements of tumor perfusion over a short time interval, we sought to investigate the evolution of tumor blood volume changes for brain metastases after SRS using this technique and to validate it against a conventional contrast enhanced perfusion technique, DCE-MRI.

## Materials and methods

### Subjects

We conducted a prospective study approved by our research ethics board. Inclusion criteria were: age ≥18 years, able to provide consent for MRI, radiographic diagnosis of brain metastases, pathologically proven primary malignancy, life expectancy greater than 6 months, a Karnofsky performance status greater than 70, and planned therapy with SRS alone. Patients with contraindication to MRI or prior allergic reaction or contraindication to MR contrast were excluded. Baseline clinical parameters were recorded including age, gender, radiation dose, steroid dose, recursive partitioning analysis score, Karnofsky performance status, Eastern Cooperative Oncology Group performance status, and whether extracranial disease was stable or progressing. SRS was delivered using a linear-accelerator in accordance with RTOG 9005 [20]. Biologically effective dose was calculated based on the generalized linear-quadratic model [21]. To control for any confounding effects of steroids, the patient's pre-SRS dose was maintained until the 1 week post-treatment MRI was performed.

### MRI acquisition

MRI was obtained at baseline (within 10 days prior to SRS), 1 week post-SRS and 1 month post-SRS. MRI was performed at 3 T (Achieva, Philips Healthcare, Best, Netherlands) using an 8 channel head coil. Diffusion MR was acquired using a Stejskal–Tanner diffusion-weighted EPI spin-echo pulse sequence [22], with diffusion-weighting obtained along 3 orthogonal directions using 6 different $b$ values ($b$=0, 200, 400, 600, 800, 1000s/mm$^2$). Images were acquired in the axial plane with in plane resolution of 1.2×1.2 mm$^2$, slice thickness=5 mm (no inter-slice gap), NEX=1, TR=5950 ms, TE=61 ms, echo train length=87, flip angle=90°. DCE-MRI was acquired in the sagittal plane using 3D fast field echo (FFE) sequence with in plane resolution of 1×1 mm$^2$, slice thickness=8 mm, NEX=1, TR=4 ms, TE=2.02 ms, flip angle=15°, temporal resolution=5.2 s, number of time points=60 after intravenous injection of a bolus of contrast agent (gadobutrol, Bayer Inc., Toronto) at a dose of 0.1 mmol/kg followed by a 20 mL saline flush. 3D T1 weighted FSPGR images were acquired in the axial plane for tumor co-registration with in plane resolution of 1×1.1 mm$^2$, slice thickness=1.5 mm, NEX=1, TR=9.5 ms, TE=2.3 ms, and flip angle=8°. Follow-up clinical MRI after 1 month was obtained for most patients and included the 3D T1 weighted FSPGR sequence for tumor volume assessment.

### DCE pharmacokinetic modelling

Pharmacokinetic analysis was performed on DCE-MRI data using the two compartment extended Tofts–Kety model [23]. In order to ensure accuracy and consistency of the analysis, the input function was measured from an ROI manually drawn on the internal carotid artery. $K^{trans}$ is the volume transfer constant describing the rate by which contrast diffuses from the plasma space into the extravascular extracellular space, $v_e$ is the extravascular extracellular space volume fraction per unit volume of tissue, and $v_p$ is the blood plasma space per unit volume of tissue.

### IVIM theory

The diffusion signal for a tissue can be modeled in a biexponential manner as the sum of the signal arising from intravascular and extravascular water compartments according to the IVIM model first proposed by Le Bihan et al. [24]:

$$\frac{S(b)}{S_0} = f \cdot e^{-bD*} + (1-f) \cdot e^{-bD} \quad (1)$$

Here, $f$ (also known as the perfusion fraction) represents the fraction of MR detectable water in the intravascular compartment and is proportional to blood volume [14]. $1-f$ represents the fraction of slower moving water, corresponding to extravascular water. $D^*$ and $D$ are the pseudodiffusion and true diffusion coefficients respectively and measure the average motion of water in each compartment. For $b > 200$, signal from the intravascular compartment approaches zero and the first term in Eq. 1 becomes negligible [25] allowing the following simplification:

$$\ln\left(\frac{S(b)}{S_0}\right) = -bD + \ln(1-f) \quad (2)$$

Equation 2 shows a linear relationship between the natural log of diffusion signal and $b$, and allows a solution of $D$ and $f$ from the slope and y-intercept of this relationship respectively at the expense of $D^*$. This simplified methodology, also referred to as asymptotic fitting, was first described by Le Bihan [24] and later by others [26, 27] and has been validated against conventional bi-exponential fitting methodologies for primary brain tumors [28].

### Image analysis

Maps of $v_p$, $K^{trans}$, $v_e$, $ADC$, and $f$ were calculated using custom-written scripts (Matlab, Optimization Toolbox; Mathworks, Natick, Mass). Calculated maps were co-registered to gadolinium-enhanced 3D T1-weighted images using the local Pearson correlation method [29]. A 12 degree of freedom affine transformation was applied in order to minimize susceptibility related geometric distortions in the EPI data. Volumetric ROIs were traced for each tumor on the post-gadolinium T1-weighted images, excluding necrotic/non-enhancing tumor components. Tumor ROIs were then used to extract the mean value of each parameter at baseline, 1 week and 1 month post SRS. Tumor ROIs were also placed surrounding the entire tumor (including both enhancing and non-enhancing components) to calculate total tumor volume, which was used to calculate tumor volume change between last follow-up MRI (>1 month) and baseline MRI. For these tumors, radiographic response was graded using a previously described scale [30] where complete response (CR) is 100% decrease in tumor volume, partial response (PR) is ≥58.5% decrease, stable disease (SD) is <58.5% decrease and <71.5% increase, and progressive disease (PD) is ≥71.5% increase. Responders were defined as tumors showing CR or PR and non-responders defined as tumors showing SD or PD. Tumors were excluded if they contained gross haemorrhage detected on $b=0$ DWI images.

### Statistical analysis

Statistical analysis was performed in Prism Version 6.0 (GraphPad Software, La Jolla, CA). Comparison of baseline, 1 week and 1 month values for $v_p$, $K^{trans}$, $v_e$, $ADC$, and $f$ were made using paired $t$ test. Percentage Change in $v_p$ and $f$ at 1 month compared to baseline was calculated and unpaired $t$ test was used to compare these changes for responders and non-responders. Statistical significance was defined as $p < 0.05$. Linear regression of $f$ and $v_p$ was performed and Pearson correlation coefficient was calculated.

## Results

Fifteen patients with a total of 20 tumors were analyzed (Table 1). All patients were treated with SRS alone. There was extended follow-up beyond 1 month for eleven patients (15 tumors) with a mean follow-up of 220 days (range 59–408 days). Of the tumors with follow-up greater than 1 month, 3 showed CR (100% decrease in volume), 3 showed PR (mean = 86% decrease, σ = 9%) and 6 showed SD (mean = 23% decrease, σ = 22%). Only 3 tumors showed radiographic evidence of PD (mean = 975% increase in volume, σ = 1476%); however, there was no pathological specimen to determine if these were the result of treatment effects or tumor recurrence. 5 tumors did not have extended follow-up past 1 month.

Figure 1 shows $v_p$, $K^{trans}$, $ADC$, and $f$ maps at baseline for a typical metastasis. Table 2 summarizes changes in perfusion parameters for all tumors. There was a statistically significant decrease in $v_p$ from baseline to 1 month post SRS and from 1 week to 1 month (paired $t$ test, $p = 0.0002$ and 0.002 respectively) (Fig. 2). No significant change in $v_p$ was observed between baseline and 1 week (paired $t$ test, $p = 0.41$). $K^{trans}$ showed a statistically significant decrease from baseline to 1 month and 1 week to 1 month (paired $t$ test, $p = 0.0002$ and 0.0001 respectively). No significant change in $K^{trans}$ was observed between baseline and 1 week (paired $t$ test, $p = 0.4$). $f$ showed a significant increase from baseline to 1 month and from 1 week to 1 month (paired $t$ test, $p = 0.03$ and 0.04 respectively) (Fig. 2). No significant change in mean $f$ was observed from baseline to 1 week (paired $t$ test, $p = 0.81$). $v_e$ and $ADC$ showed no significant change.

For tumors with follow-up greater than 1 month, responders (CR + PR) and non-responders (SD + PD) both showed reduction in $v_p$ at 1 month compared to baseline (−58.3% and −49.3% respectively) which was not significantly different (unpaired $t$ test, $p = 0.6$). Responders and non-responders both demonstrated an increase in $f$ at 1 month compared to baseline (+32.3% and +10%

**Table 1** Patient demographics and tumor characteristics

| Age/Sex | Primary | Location | Dose (cGy) | Follow-up (days) | % Volume change | Response |
|---|---|---|---|---|---|---|
| 48/M | Lung | Frontal lobe | 2000 | 408 | −100 | CR |
| 68/F | Lung | Temporal lobe | 1800 | 371 | +90 | PD |
| 77/F | Breast | Frontal lobe | 1800 | 26 | | |
| 57/F | Lung | Occipital lobe | 1800 | 354 | −100 | CR |
| 57/F | Breast | Parietal lobe | 1800 | 34 | | |
| | | Parietal lobe | 1800 | | | |
| 64/F | Lung | Frontal lobe | 1800 | 200 | −83 | PR |
| 80/F | Lung | Parietal lobe | 1800 | 206 | −96 | PR |
| | | Parietal lobe | 2000 | | −79 | PR |
| 65/F | Lung | Parietal lobe | 1600 | 209 | −22 | SD |
| 62/F | Colorectal | Occipital lobe | 2000 | 32 | | |
| 45/F | Breast | Occipital lobe | 2000 | 90 | −100 | CR |
| 63/M | Lung | Cerebellum | 1800 | 88 | +1 | SD |
| | | Frontal lobe | 1800 | | +4 | SD |
| | | Occipital lobe | 2000 | | −39 | SD |
| | | Parietal lobe | 2000 | | −27 | SD |
| 58/F | Breast | Frontal lobe | 2000 | 279 | +2680 | PD |
| 51/F | Breast | Temporal lobe | 1800 | 59 | +155 | PD |
| 85/M | Colorectal | Frontal lobe | 2000 | 29 | | |
| 68/M | Lung | Cerebellum | 1800 | 157 | −52 | SD |

respectively) which was also not significantly different (unpaired *t* test, p = 0.3).

The relationship between *f* and $v_p$ is shown for tumors (Fig. 3) and fitted to a linear regression. There was a weak correlation between these parameters at baseline (r = 0.33), 1 week (r = 0.14) and 1 month after treatment (r = 0.30).

## Discussion

We present the first study evaluating perfusion changes for brain metastases in the first month after SRS using IVIM and validated against DCE-MRI. IVIM has recently seen increasing application in CNS oncology. The IVIM perfusion fraction (*f*) is a convenient measure of tumor blood volume and has shown correlation with microvessel density in animal tumor models [31]. The technique has also shown utility in distinguishing between low and high grade gliomas [32, 33], prognostication in patients with gliomas [34], and utility in distinguishing between different brain malignancies [35, 36]. To our knowledge, there has only been one prior study examining IVIM perfusion measurements in brain tumors post radiation treatment and this study examined *f* and DSC derived CBV measurements for brain metastases several months after treatment in order to distinguish between tumor recurrence and treatment effects [18].

We demonstrated a significant reduction in $v_p$ at 1 month after SRS which is consistent with the expected radiobiology of SRS. The result is also consistent with previously published studies examining perfusion changes after SRS. For example, Essig et al. examined perfusion changes in brain metastases treated with SRS using DSC perfusion [8]. In that study of 18 brain metastases treated with SRS alone, reductions in CBV were found for tumor responders and stable disease measured at 6 weeks post SRS. The reduction in tumor perfusion found with DCE-MRI in our study is also concordant with a previous study showing a reduction in tumor blood flow in metastases treated with SRS at 6 weeks post-therapy using both DSC and arterial spin labeling (ASL). The reduction in $K^{trans}$ observed in our study is also consistent with a reduction in tumor blood flow as $K^{trans}$ in tumors reflects both tumor blood flow and vascular permeability [37].

IVIM measurements of tumor blood volume (*f*) showed a significant increase at 1 month which was contradictory to the finding of decreased $v_p$ found with DCE-MRI. One possible explanation for this discordant behaviour is related to differences in the type of perfusion that DCE-MRI and IVIM measure. Contrast enhanced perfusion techniques measure total tumor blood volume within all vasculature of a tumor regardless of size of vessels within the vascular bed. The IVIM perfusion fraction, on the other hand, is less sensitive to water in larger conducting vessels and more sensitive to water within the microvasculature [31, 38]. It has been shown that *f* correlates well with microvessel density measured by CD31 immunohistochemistry in mouse

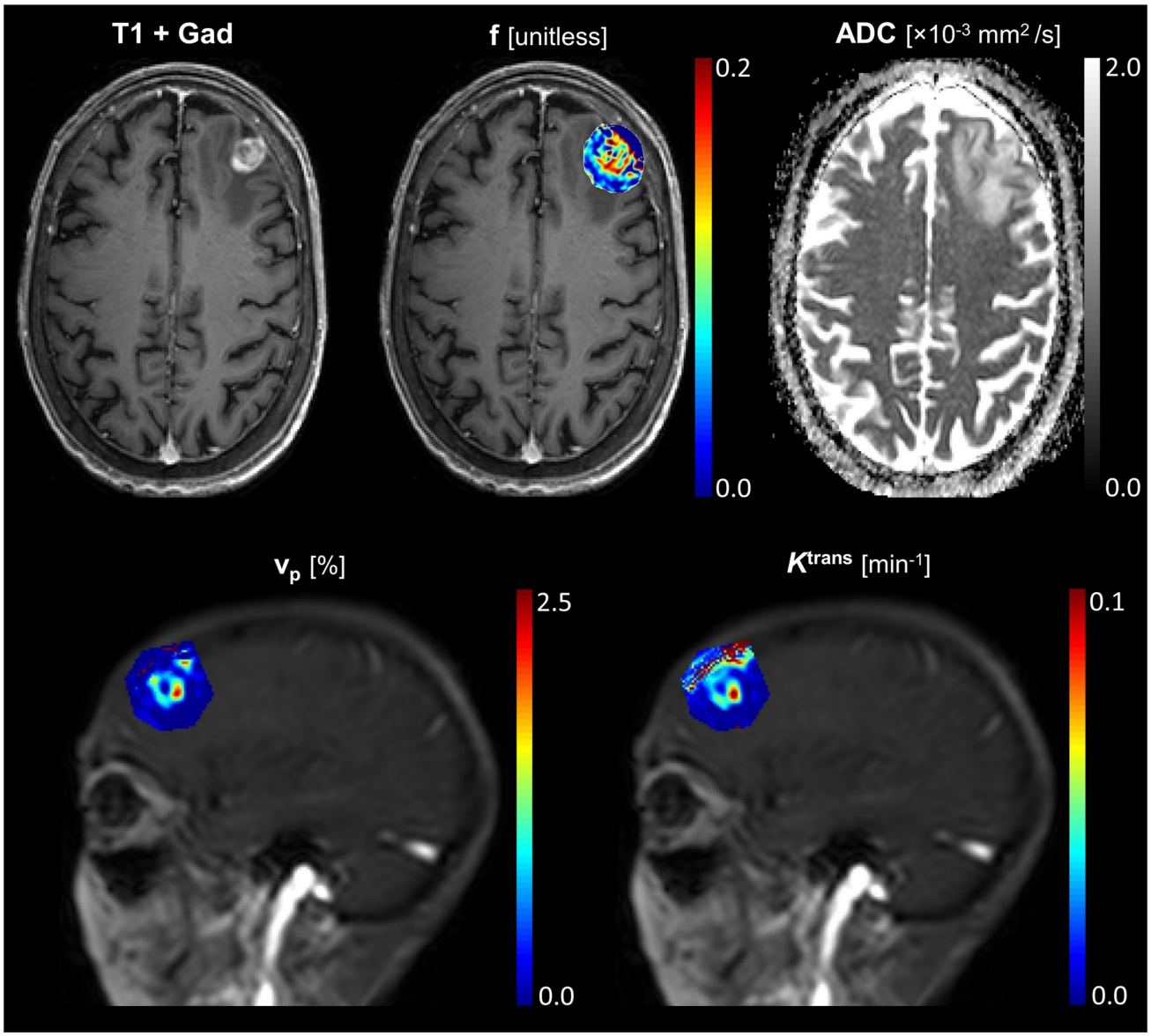


**Fig. 1** IVIM and DCE-MRI maps for a typical metastasis at baseline. Axial contrast enhanced T1-weighted image shows a centrally necrotic metastasis in left frontal lobe (*left top row*). Perfusion fraction (f) map overlayed on post-contrast image (*center top row*) shows elevated f in the periphery of the metastasis. The ADC map (*right top row*) shows elevated diffusivity for the metastasis and vasogenic edema in the surround brain. DCE-MRI $v_p$ and $K^{trans}$ maps (*bottom row*) of the same metastasis in the sagittal plane show elevated values in the periphery of the tumor

**Table 2** Summary of DCE-MRI and IVIM parameters

| | Baseline (mean ± SD) | 1 Week (mean ± SD) | 1 Month (mean ± SD) | Baseline versus 1 week (p value) | Baseline versus 1 month (p value) | 1 Week versus 1 month (p value) |
|---|---|---|---|---|---|---|
| $v_p$ (%) | 3.7 ± 2.3 | 3.3 ± 2.7 | 2.1 ± 2.4 | 0.41 | 0.0002* | 0.002* |
| $K^{trans}$ ($min^{-1}$) | 0.068 ± 0.036 | 0.061 ± 0.034 | 0.037 ± 0.021 | 0.40 | 0.0002* | 0.0001* |
| $v_e$ (%) | 10.8 ± 5.4 | 10.6 ± 4.4 | 10.0 ± 6.2 | 0.87 | 0.48 | 0.73 |
| *ADC* ($10^{-3}$ $mm^2$/s) | 1.1 ± 0.16 | 1.1 ± 0.15 | 1.1 ± 0.22 | 0.33 | 0.90 | 0.57 |
| *f* (unitless) | 0.083 ± 0.024 | 0.084 ± 0.026 | 0.10 ± 0.028 | 0.81 | 0.03* | 0.04* |

p values for paired *t* test. Statistically significant results ($p < 0.05$)*

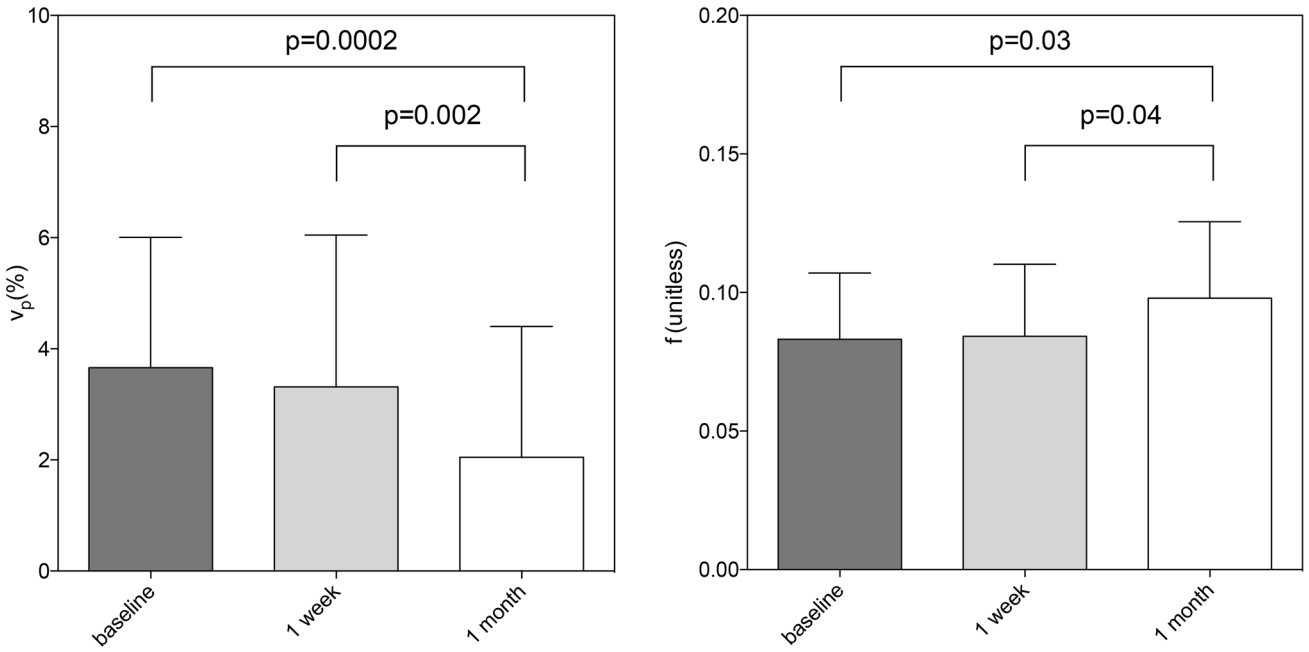


**Fig. 2** Temporal evolution of mean plasma fraction ($v_p$) (*left panel*) and f (*right panel*) for metastases (*error bars* represent standard deviation). Statistically significant decrease in $v_p$ was found at 1 month (paired *t* test). A statistically significant increase in f was found at 1 month (paired *t* test)

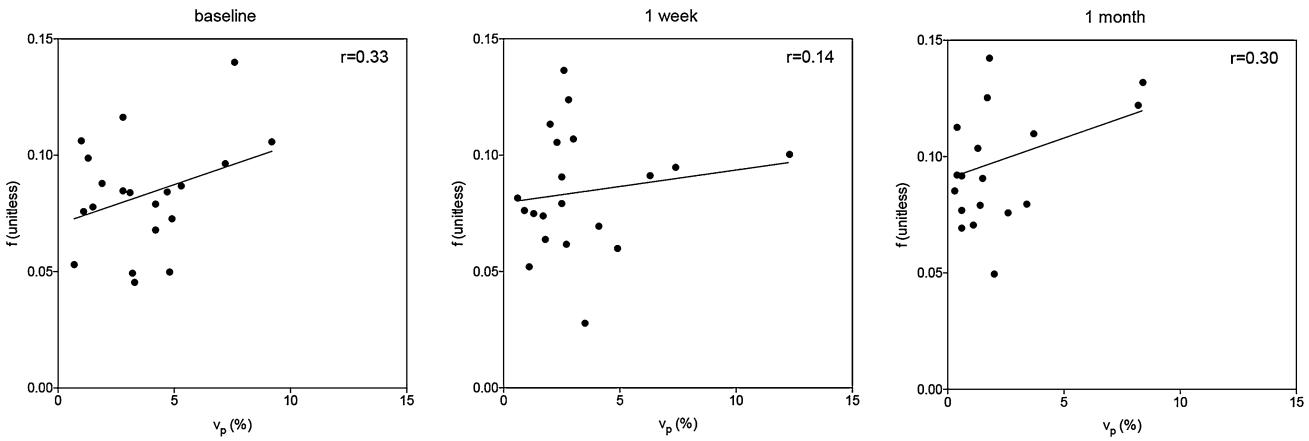


**Fig. 3** Correlation between IVIM perfusion fraction (f) and plasma fraction ($v_p$) for all tumors at baseline (*left panel*), 1 week (*middle panel*), and 1 month post SRS (*right panel*). Each point represents the mean f or $v_p$ over the tumor ROI and data is fitted with a linear regression. There is weak correlation between IVIM and DCE perfusion measurements of blood volume at baseline and after SRS. The correlation coefficient (r) is indicated for each

heterotopic colorectal tumor model [31]. The observed increase in *f* may therefore relate to an increase in vasculogenesis and microvessel density occurring after radiation therapy [3].

An alternative explanation for the increase in *f* is related to violation of assumptions made in the IVIM model that might occur after radiation therapy. The classic IVIM equation is based on an assumption of two tissue compartments (intravascular and extravascular) which may not be an accurate representation of tissues [39]. After SRS, increased vascular and cell membrane permeability will result in a more complex multicompartmental tumor microenvironment which is probably not adequately represented by two tissue compartments. In the post-SRS case, an increase in *f* measured using the assumption of a two compartment diffusion model could therefore reflect an increase in the amount of more mobile extravascular–extracellular water in the tumor after SRS rather than an increase in

blood volume. Evidence for increasing extravascular extracellular volume after SRS has been shown by the diffusion experiments of Mardor et al. examining brain tumors (primary and metastatic) treated with SRS or fractionated radiation therapy [40]. In that study, the diffusion signal of tumors was measured with 14 *b*-values from $b = 250–4000$ modeled as a bi-exponential consisting of two water compartments undergoing either fast or slow motion. Using a biexponential fit, the authors found that after treatment with SRS, the volume corresponding to the slow compartment (thought to represent intracellular water signal) decreased and there was corresponding increase in the compartment undergoing faster motion (thought mainly to represent extracellular water). Our study, however, failed to show any significant increase in $v_e$ or *ADC* to confirm this possibility.

Another assumption of the IVIM model that could lead to deviations between IVIM and contrast enhanced perfusion techniques is the assumption that the T2 relaxivity between intravascular and extravascular compartments is unaltered after treatment. After radiation treatment, the relative T2 relaxivities of the intravascular and extravascular compartment can change significantly which will affect *f* independent of a change in tumor blood volume. This explanation was recently invoked in a study examining IVIM perfusion in rectal cancers treated with radiation in which the authors failed to show any significant change in *f* after combined chemoradiation [41].

One of the limitations of this study is the use of a simplified version of IVIM based on asymptotic fitting model. Previous work, however, has demonstrated no significant difference in *f* measured using conventional IVIM and this simplified model for primary brain tumors [28]. In fact, the asymptotic fitting model has been shown by others to provide better correlation between IVIM and DCE-MRI perfusion parameters compared to the conventional bi-exponential diffusion model in head and neck squamous cell carcinoma [42]. Another limitation of this study was the small number of tumors with extended follow-up. Both responders and non-responders showed a similar trend in perfusion parameters at 1 month compared to baseline which was not significantly different. Further work with a larger sample size is needed to determine if changes in DCE-MRI or IVIM perfusion parameters at 1 month can predict long term response of brain metastases to SRS.

There is great disparity in the literature regarding the correlation between measures of blood volume using contrast enhanced techniques and IVIM in brain tumors. In some studies, a moderate correlation between these two techniques was found [15, 28], whilst in other studies, weak to no correlation was observed [43]. The weak correlation between *f* and $v_p$ found in this study again raises doubts regarding the equivalence of DCE-MRI and IVIM measurements of blood volume. Whether this reflects a difference in the type of perfusion information IVIM is measuring (e.g. microvessel density or blood volume related to the microcirculation) or a limitation in the IVIM model is an ongoing question that will require further study.

## Conclusion

In summary, we have characterized changes in perfusion for brain metastases in the first month after SRS using IVIM and DCE-MRI. IVIM and DCE-MRI measures of tumor blood volume show no significant change 1 week post-treatment. A significant decrease in blood volume at 1 month was observed using DCE-MRI which is consistent with the radiobiology of SRS and prior MR perfusion studies. IVIM measures of tumor blood volume show contradictory behaviour with significant increase in blood volume at 1 month. The reason for the discrepancy between DCE-MRI and IVIM is unclear and caution is therefore needed when interpreting IVIM measures of tumor perfusion in the early period after SRS until further research is performed.

**Funding** The authors received no financial support for the research, authorship, and/or publication of this article.

**Compliance with ethical standards**

**Conflict of interest** The authors report no conflict of interest related to this article.

**Ethical approval** Informed consent was obtained and the study was conducted in accordance with the ethical standards of the institutional REB.

## References

1. Brown PD, Jaeckle K, Ballman KV, Farace E, Cerhan JH, Anderson SK, Carrero XW, Barker FG 2nd, Deming R, Burri SH, Menard C, Chung C, Stieber VW, Pollock BE, Galanis E, Buckner JC, Asher AL (2016) Effect of radiosurgery alone vs radiosurgery with whole brain radiation therapy on cognitive function in patients with 1 to 3 brain metastases: a randomized clinical trial. JAMA 316(4):401–409. doi:10.1001/jama.2016.9839
2. Brurberg KG, Thuen M, Ruud EB, Rofstad EK (2006) Fluctuations in $pO_2$ in irradiated human melanoma xenografts. Radiat Res 165(1):16–25
3. Kioi M, Vogel H, Schultz G, Hoffman RM, Harsh GR, Brown JM (2010) Inhibition of vasculogenesis, but not angiogenesis, prevents the recurrence of glioblastoma after irradiation in mice. J Clin Invest 120(3):694–705. doi:10.1172/JCI40283
4. Mantyla MJ, Toivanen JT, Pitkanen MA, Rekonen AH (1982) Radiation-induced changes in regional blood flow in human tumors. Int J Radiat Oncol Biol Phys 8(10):1711–1717
5. Pirhonen JP, Grenman SA, Bredbacka AB, Bahado-Singh RO, Salmi TA (1995) Effects of external radiotherapy on uterine blood flow in patients with advanced cervical carcinoma assessed by color Doppler ultrasonography. Cancer 76(1):67–71

6. Kocher M, Treuer H, Voges J, Hoevels M, Sturm V, Muller RP (2000) Computer simulation of cytotoxic and vascular effects of radiosurgery in solid and necrotic brain metastases. Radiother Oncol 54(2):149–156
7. Kirkpatrick JP, Meyer JJ, Marks LB (2008) The linear-quadratic model is inappropriate to model high dose per fraction effects in radiosurgery. Semin Radiat Oncol 18(4):240–243. doi:10.1016/j.semradonc.2008.04.005
8. Essig M, Waschkies M, Wenz F, Debus J, Hentrich HR, Knopp MV (2003) Assessment of brain metastases with dynamic susceptibility-weighted contrast-enhanced MR imaging: initial results. Radiology 228(1):193–199. doi:10.1148/radiol.2281020298
9. Weber MA, Thilmann C, Lichy MP, Gunther M, Delorme S, Zuna I, Bongers A, Schad LR, Debus J, Kauczor HU, Essig M, Schlemmer HP (2004) Assessment of irradiated brain metastases by means of arterial spin-labeling and dynamic susceptibility-weighted contrast-enhanced perfusion MRI: initial results. Invest Radiol 39(5):277–287
10. Huang J, Wang AM, Shetty A, Maitz AH, Yan D, Doyle D, Richey K, Park S, Pieper DR, Chen PY, Grills IS (2011) Differentiation between intra-axial metastatic tumor progression and radiation injury following fractionated radiation therapy or stereotactic radiosurgery using MR spectroscopy, perfusion MR imaging or volume progression modeling. Magn Reson Imaging 29(7):993–1001. doi:10.1016/j.mri.2011.04.004
11. Lin Y, Li J, Zhang Z, Xu Q, Zhou Z, Zhang Z, Zhang Y, Zhang Z (2015) Comparison of intravoxel incoherent motion diffusion-weighted mr imaging and arterial spin labeling MR imaging in gliomas. Biomed Res Int 2015:234245. doi:10.1155/2015/234245
12. Mazhar SM, Shiehmorteza M, Kohl CA, Middleton MS, Sirlin CB (2009) Nephrogenic systemic fibrosis in liver disease: a systematic review. J Magn Reson Imaging 30(6):1313–1322. doi:10.1002/jmri.21983
13. Le Bihan D (1988) Intravoxel incoherent motion imaging using steady-state free precession. Magn Reson Med 7(3):346–351
14. Le Bihan D, Turner R (1992) The capillary network: a link between IVIM and classical perfusion. Magn Reson Med 27(1):171–178
15. Federau C, Meuli R, O'Brien K, Maeder P, Hagmann P (2014) Perfusion measurement in brain gliomas with intravoxel incoherent motion MRI. AJNR Am J Neuroradiol 35(2):256–262. doi:10.3174/ajnr.A3686
16. Bisdas S, Koh TS, Roder C, Braun C, Schittenhelm J, Ernemann U, Klose U (2013) Intravoxel incoherent motion diffusion-weighted MR imaging of gliomas: feasibility of the method and initial results. Neuroradiology 55(10):1189–1196. doi:10.1007/s00234-013-1229-7
17. Kim HS, Suh CH, Kim N, Choi CG, Kim SJ (2014) Histogram analysis of intravoxel incoherent motion for differentiating recurrent tumor from treatment effect in patients with glioblastoma: initial clinical experience. AJNR Am J Neuroradiol 35(3):490–497. doi:10.3174/ajnr.A3719
18. Kim DY, Kim HS, Goh MJ, Choi CG, Kim SJ (2014) Utility of intravoxel incoherent motion MR imaging for distinguishing recurrent metastatic tumor from treatment effect following gamma knife radiosurgery: initial experience. AJNR Am J Neuroradiol 35(11):2082–2090. doi:10.3174/ajnr.A3995
19. Joo I, Lee JM, Grimm R, Han JK, Choi BI (2016) Monitoring vascular disrupting therapy in a rabbit liver tumor model: relationship between tumor perfusion parameters at IVIM diffusion-weighted MR imaging and those at dynamic contrast-enhanced MR imaging. Radiology 278(1):104–113. doi:10.1148/radiol.2015141974
20. Shaw E, Scott C, Souhami L, Dinapoli R, Kline R, Loeffler J, Farnan N (2000) Single dose radiosurgical treatment of recurrent previously irradiated primary brain tumors and brain metastases: final report of RTOG protocol 90-05. Int J Radiat Oncol Biol Phys 47(2):291–298
21. Brenner DJ (2008) The linear-quadratic model is an appropriate methodology for determining isoeffective doses at large doses per fraction. Semin Radiat Oncol 18(4):234–239. doi:10.1016/j.semradonc.2008.04.004
22. Turner R, Le Bihan D, Maier J, Vavrek R, Hedges LK, Pekar J (1990) Echo-planar imaging of intravoxel incoherent motion. Radiology 177(2):407–414. doi:10.1148/radiology.177.2.2217777
23. Tofts PS, Brix G, Buckley DL, Evelhoch JL, Henderson E, Knopp MV, Larsson HB, Lee TY, Mayr NA, Parker GJ, Port RE, Taylor J, Weisskoff RM (1999) Estimating kinetic parameters from dynamic contrast-enhanced T(1)-weighted MRI of a diffusable tracer: standardized quantities and symbols. J Magn Reson Imaging 10(3):223–232
24. Le Bihan D, Breton E, Lallemand D, Aubin ML, Vignaud J, Laval-Jeantet M (1988) Separation of diffusion and perfusion in intravoxel incoherent motion MR imaging. Radiology 168(2):497–505. doi:10.1148/radiology.168.2.3393671
25. Le Bihan D, Turner R, MacFall JR (1989) Effects of intravoxel incoherent motions (IVIM) in steady-state free precession (SSFP) imaging: application to molecular diffusion imaging. Magn Reson Med 10(3):324–337
26. Pekar J, Moonen CT, van Zijl PC (1992) On the precision of diffusion/perfusion imaging by gradient sensitization. Magn Reson Med 23(1):122–129
27. Wirestam R, Borg M, Brockstedt S, Lindgren A, Holtas S, Stahlberg F (2001) Perfusion-related parameters in intravoxel incoherent motion MR imaging compared with CBV and CBF measured by dynamic susceptibility-contrast MR technique. Acta Radiol 42(2):123–128
28. Conklin J, Heyn C, Roux M, Cerny M, Wintermark M, Federau C (2016) A simplified model for intravoxel incoherent motion perfusion imaging of the brain. AJNR Am J Neuroradiol. doi:10.3174/ajnr.A4929
29. Saad ZS, Glen DR, Chen G, Beauchamp MS, Desai R, Cox RW (2009) A new method for improving functional-to-structural MRI alignment using local Pearson correlation. Neuroimage 44(3):839–848. doi:10.1016/j.neuroimage.2008.09.037
30. Follwell MJ, Khu KJ, Cheng L, Xu W, Mikulis DJ, Millar BA, Tsao MN, Laperriere NJ, Bernstein M, Sahgal A (2012) Volume specific response criteria for brain metastases following salvage stereotactic radiosurgery and associated predictors of response. Acta Oncol 51(5):629–635. doi:10.3109/0284186X.2012.681066
31. Lee HJ, Rha SY, Chung YE, Shim HS, Kim YJ, Hur J, Hong YJ, Choi BW (2014) Tumor perfusion-related parameter of diffusion-weighted magnetic resonance imaging: correlation with histological microvessel density. Magn Reson Med 71(4):1554–1558. doi:10.1002/mrm.24810
32. Hu YC, Yan LF, Wu L, Du P, Chen BY, Wang L, Wang SM, Han Y, Tian Q, Yu Y, Xu TY, Wang W, Cui GB (2014) Intravoxel incoherent motion diffusion-weighted MR imaging of gliomas: efficacy in preoperative grading. Sci Rep 4:7208. doi:10.1038/srep07208
33. Togao O, Hiwatashi A, Yamashita K, Kikuchi K, Mizoguchi M, Yoshimoto K, Suzuki SO, Iwaki T, Obara M, Van Cauteren M, Honda H (2016) Differentiation of high-grade and low-grade diffuse gliomas by intravoxel incoherent motion MR imaging. Neuro Oncol 18(1):132–141. doi:10.1093/neuonc/nov147
34. Federau C, Cerny M, Roux M, Mosimann PJ, Maeder P, Meuli R, Wintermark M (2016) IVIM perfusion fraction is prognostic

for survival in brain glioma. Clin Neuroradiol. doi:10.1007/s00062-016-0510-7
35. Suh CH, Kim HS, Lee SS, Kim N, Yoon HM, Choi CG, Kim SJ (2014) Atypical imaging features of primary central nervous system lymphoma that mimics glioblastoma: utility of intravoxel incoherent motion MR imaging. Radiology 272(2):504–513. doi:10.1148/radiol.14131895
36. Shim WH, Kim HS, Choi CG, Kim SJ (2015) Comparison of apparent diffusion coefficient and intravoxel incoherent motion for differentiating among glioblastoma, metastasis, and lymphoma focusing on diffusion-related parameter. PLoS ONE 10(7):e0134761. doi:10.1371/journal.pone.0134761
37. Sourbron SP, Buckley DL (2012) Tracer kinetic modelling in MRI: estimating perfusion and capillary permeability. Phys Med Biol 57(2):R1–R33. doi:10.1088/0031-9155/57/2/R1
38. Iima M, Reynaud O, Tsurugizawa T, Ciobanu L, Li JR, Geffroy F, Djemai B, Umehana M, Le Bihan D (2014) Characterization of glioma microcirculation and tissue features using intravoxel incoherent motion magnetic resonance imaging in a rat brain model. Invest Radiol 49(7):485–490. doi:10.1097/RLI.0000000000000040
39. Henkelman RM, Neil JJ, Xiang QS (1994) A quantitative interpretation of IVIM measurements of vascular perfusion in the rat brain. Magn Reson Med 32(4):464–469
40. Mardor Y, Pfeffer R, Spiegelmann R, Roth Y, Maier SE, Nissim O, Berger R, Glicksman A, Baram J, Orenstein A, Cohen JS, Tichler T (2003) Early detection of response to radiation therapy in patients with brain malignancies using conventional and high b-value diffusion-weighted magnetic resonance imaging. J Clin Oncol 21(6):1094–1100
41. Nougaret S, Vargas HA, Lakhman Y, Sudre R, Do RK, Bibeau F, Azria D, Assenat E, Molinari N, Pierredon MA, Rouanet P, Guiu B (2016) Intravoxel incoherent motion-derived histogram metrics for assessment of response after combined chemotherapy and radiation therapy in rectal cancer: initial experience and comparison between single-section and volumetric analyses. Radiology 280(2):446–454. doi:10.1148/radiol.2016150702
42. Fujima N, Yoshida D, Sakashita T, Homma A, Tsukahara A, Tha KK, Kudo K, Shirato H (2014) Intravoxel incoherent motion diffusion-weighted imaging in head and neck squamous cell carcinoma: assessment of perfusion-related parameters compared to dynamic contrast-enhanced MRI. Magn Reson Imaging 32(10):1206–1213. doi:10.1016/j.mri.2014.08.009
43. Bisdas S, Braun C, Skardelly M, Schittenhelm J, Teo TH, Thng CH, Klose U, Koh TS (2014) Correlative assessment of tumor microcirculation using contrast-enhanced perfusion MRI and intravoxel incoherent motion diffusion-weighted MRI: is there a link between them? NMR Biomed 27(10):1184–1191. doi:10.1002/nbm.3172